CHAPTER IV
RESULTS AND DISCUSSION

4.1 Adsorbent Modification and Characterizations

4.1.1 Amount of Metal Loading

Atomic absorption spectrometer (Varian, SpectrAA 300 model) was used to determine the amount of Ni^{2+} and Cu^{2+} exchanged with cations of NaY zeolite. In the adsorption experiments, the concentration of metal solution was fixed at 0.01 mol/l and solution/adsorbent ratio was varied. The results are shown in Figure 4.1.

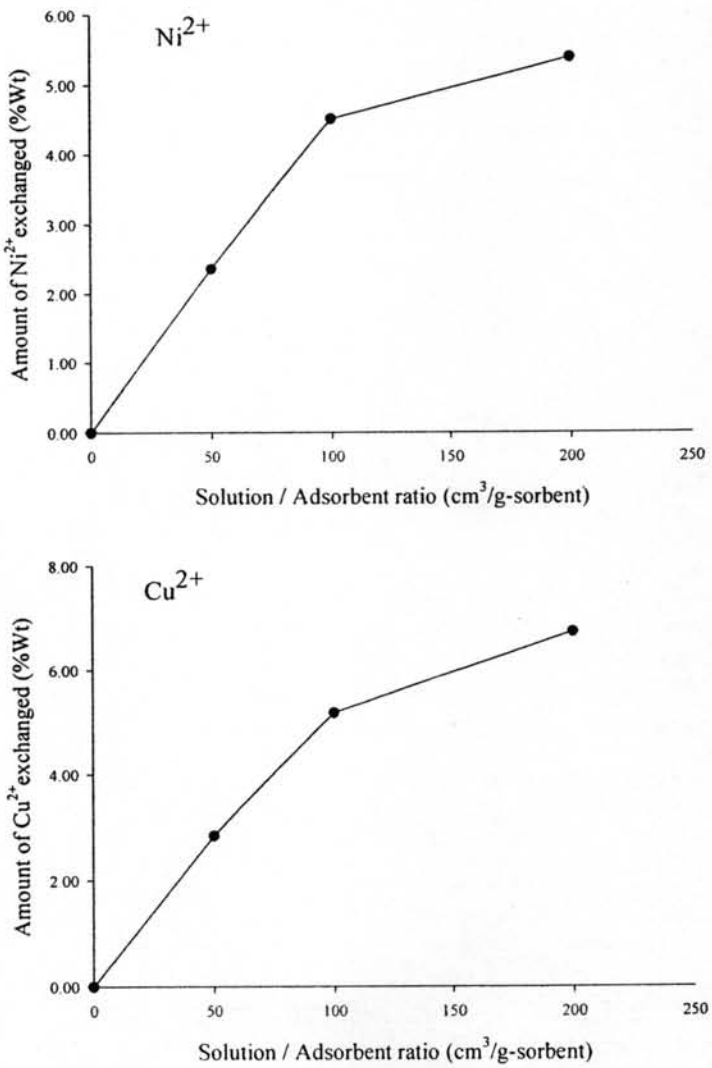

Figure 4.1 The amount of metal loading on NaY zeolite (a) Ni^{2+} (b) Cu^{2+}

As seen in Figure 4.1, the amount of Ni^{2+} and Cu^{2+} exchanged with Na^{+} in NaY zeolite increased with increasing the solution/adsorbent ratio, especially in the range of 50-100. The highest exchanged amount was observed at the solution-to-adsorbent ratio of 200 for both Ni^{2+} and Cu^{2+}, which were 5.18%wt and 6.73%wt, respectively.

4.1.2 Ion-exchange isotherm

The ion-exchange isotherm was constructed to measure a preference cation in the zeolite over another and the limitation of exchanging. In the isotherms, the equivalent fraction of the Ni^{2+} and Cu^{2+} in zeolite (E_A) and the equivalent fraction of the same cation present in solution phase ($E_{A(S)}$) were plotted as shown in Figure 4.2.

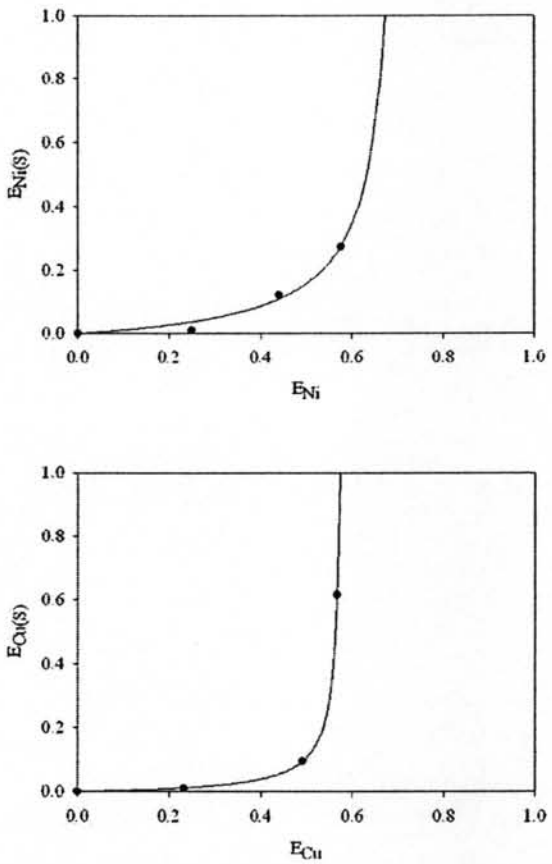

Figure 4.2 The ion-exchange isotherm for (a) Ni-Na-Y (b) Cu-Na-Y at room temperature

It can be seen that both ion-exchange isotherms of Ni^{2+} and Cu^{2+} lie under the selectivity line which draw through the point (0,0) and (1,1) which mean that the zeolite prefers the Ni^{2+} and Cu^{2+} until it reaches the maximum loading of metal. Figures 4.2a and 4.2b show that the Na^{+} in NaY zeolite can be replaced by Ni^{2+} and Cu^{2+} for 67.19% and 57.59% of the total cations, respectively. The remaining which cannot be replaced by Ni^{2+} or Cu^{2+} may cause from the size of transition metals that cannot diffuse through the pore size of zeolite to exchange with cations. However, the higher replacement of metal ions may be achieved by reexchanging that was not investigated in this study.

4.1.3 Surface Area Analysis (SAA)

The BET surface area, pore volumes and pore sizes of the structure of NaY zeolite before and after exchanged with metal ions were determined by using Sorptomatic SAA (Themo Finnigan), which are listed in Table 4.1.

Table 4.1 The BET surface area, pore volume and pore size of sorbents

Adsorbents	BET surface area (m^2/g)	Pore volume (cm^3/g)	Average pore size (Å)
NaY zeolite	538.06	123.60	6.6097
NiY zeolite (2.36%wt Ni)	482.72	110.90	8.162
NiY zeolite (4.51%wt Ni)	501.29	115.17	8.357
NiY zeolite (5.38%wt Ni)	505.97	116.24	8.762
CuY zeolite (2.83%wt Cu)	515.30	118.50	6.5341
CuY zeolite (5.18%wt Cu)	526.18	120.87	6.8547
CuY zeolite (6.73%wt Cu)	560.70	128.80	7.0836

As can be seen from the Table 4.1, the BET surface area and pore volume of NaY zeolite before and after exchanged with different amount of Ni^{2+} or Cu^{2+} were not significantly changed. This indicates that the structure of zeolite is still the same after ion exchange followed by heat treatment at 450°C.

4.1.4 X-ray Diffraction Spectroscopy (XRD)

The XRD results shown in Figure 4.3 are used to verify the structure of zeolite after ion exchange and heat treatment compared with the original structure of NaY zeolite before the modification.

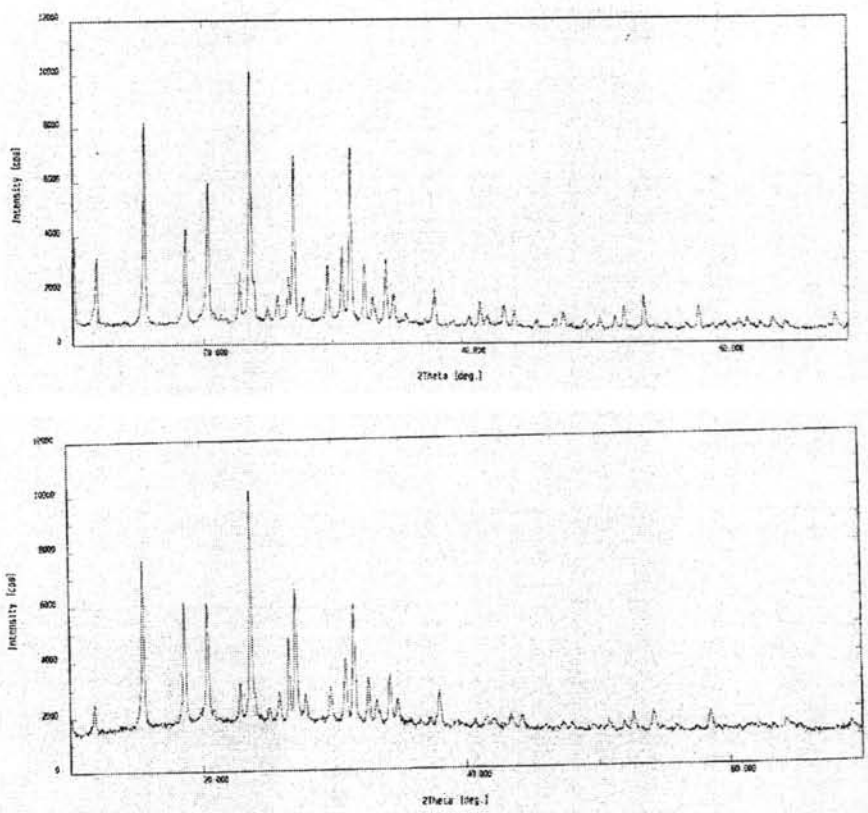

(a)

(b)

Figure 4.3 XRD patterns of ion-exchanged zeolite (a) NaY zeolite (b) NiY zeolite (Na) (5.38%wt Ni)

It can be seen in Figure 4.3 that the XRD pattern of ion-exchanged zeolite is almost similar to the XRD pattern of original structure of NaY zeolite. Therfore, it can be concluded that the structure of original NaY zeolite was still retained after ion exchanged followed by heat treatment.

4.2 Adsorption of sulfur compounds in simulated fuels

In this part of the study, decane and isooctane were used as simulated transportation fuels to represent diesel and gasoline, respectively. Sulfur compounds used were 3-metylthiophene (3-MT) and benzothiophene (BT) for isooctane and dibenzothiophene (DBT) for decane. The ratio of fuel:adsorbent was fixed at 85 (Chansa, 2004).

4.2.1 The Adsorption of Sulfur Compounds in Simulated Fuels

4.2.1.1 Adsorption of 3-methylthiophene in isooctane by NiY and CuY Zeolites

In this study, the adsorption isotherms of 3-methylthiophene in isooctane were constructed by plotting the amount of 3-methylthiophene adsorbed on zeolite and the equilibrium concentration of 3-methylthiophene in isooctane. Fuel:adsorbent ratio was fixed at 85 and the experiment was carried out at ambient condition. The results are shown in Figure 4.4 and Figure 4.5.

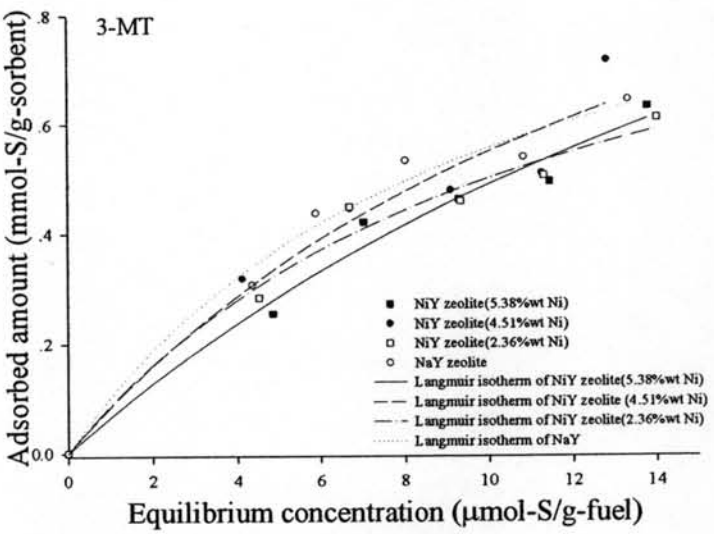

Figure 4.4 Adsorption isotherms of 3-methylthiophene in isooctane by Y zeolite with different amount of Ni^{2+} loading

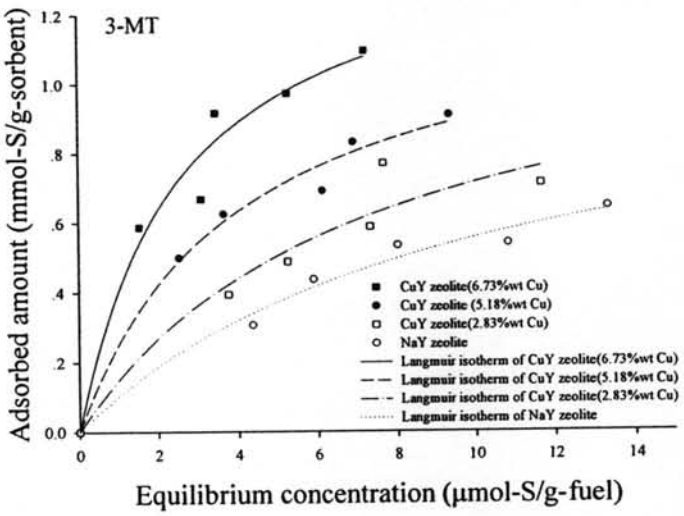

Figure 4.5 Adsorption isotherms of 3-methylthiophene in isooctane by Y zeolite with different amount of Cu^{2+} loading

The experimental data of the adsorption of 3-MT in isooctane on NiY and CuY zeolites were found to be well fitted with Langmuir isotherm as illustrated by this equation:

$$q = \frac{q_{\max} k C_e}{1 + k C_e}$$

where q and q_{max} are the amount of adsorbed and maximum adsorption capacity, respectively. C_e are the equilibrium concentration. The adsorption equilibrium constant (k) expresses the affinity between the adsorbate and adsorbent. The Langmuir parameters are shown in Table 4.2 for NiY zeolite and Table 4.3 for CuY zeolite. From the adsorption isotherms of 3-MT in isooctane by NiY zeolite, their k values were slightly different when varying the amount of Ni^{2+} loading on zeolite while the adsorption capacities increased. On the contrary for CuY zeolite isotherms, when increasing the amount of metal loading, the k values of 3-MT adsorbed on CuY zeolite significantly increase and maximum capacities also increased. Even though the maximum capacity in adsorbing 3-MT in isooctane of NiY and CuY was not much different, but the k values from CuY zeolite isotherms were much higher than NiY which indicates that 3-MT had higher affinity with CuY zeolite than with NiY zeolite.

Table 4.2 Maximum capacity and adsorption constant of the adsorption of 3-methylthiophene in isooctane by NiY zeolite with different Ni^{2+} loading

Adsorbent	q_{max} (mmol-S/g-orbent)	k (g-fuel/μmol-S)
NiY (2.36%wt Ni)	1.064	0.089
NiY (4.51%wt Ni)	1.425	0.063
NiY (5.38%wt Ni)	1.717	0.040
NaY	1.097	0.102

Table 4.3 Maximum capacity and adsorption constant of the adsorption of 3-methylyhiophene in isooctane by CuY zeolite with different Cu^{2+} loading

Adsorbent	q_{max} (mmol-S/g-orbent)	k (g-fuel/μmol-S)
CuY (2.83%wt Cu)	1.227	0.139
CuY (5.18%wt Cu)	1.273	0.246
CuY (6.73%wt Cu)	1.472	0.379
NaY	1.097	0.102

4.2.1.2 Adsorption of benzothiophene in isooctane by NiY and CuY zeolites

The adsorption isotherms of benzothiophene by NiY and CuY were constructed by plotting the amount of benzothiophene adsorbed on zeolite and equilibrium concentration of benzothiophene in isooctane. Fuel:adsorbent ratio was fixed at 85 and the experiment was carried out at ambient condition. The results are shown in Figure 4.6 and Figure 4.7.

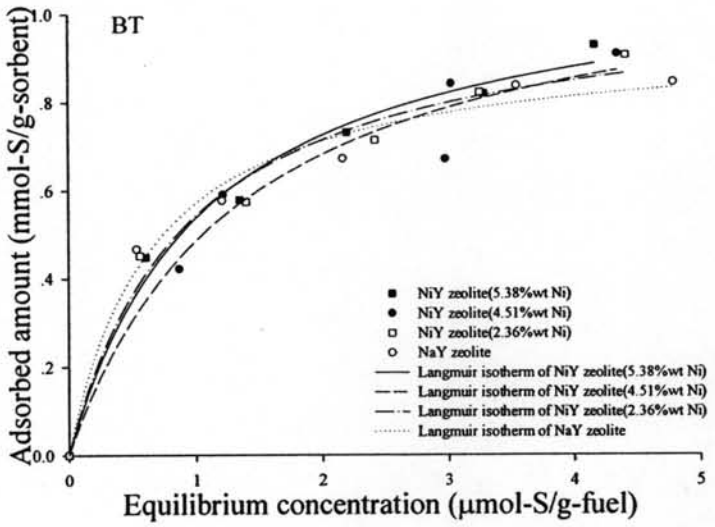

Figure 4.6 Adsorption of benzothiophene in isooctane by NiY zeolite with different amount of Ni^{2+} loading

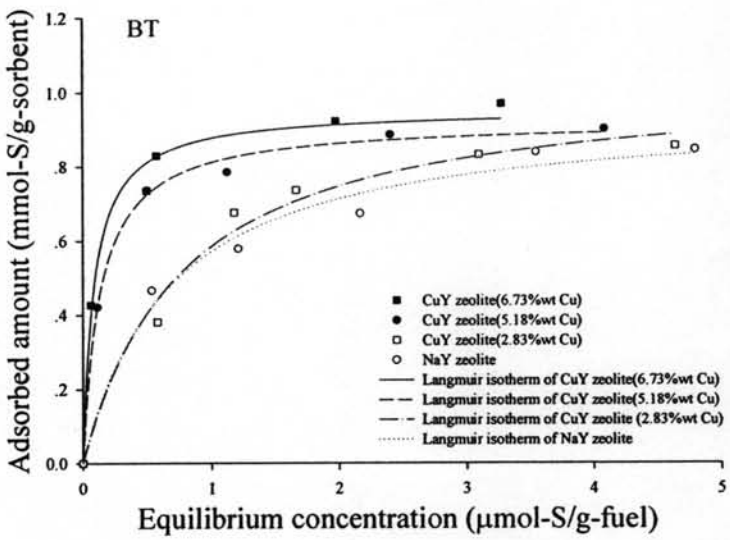

Figure 4.7 Adsorption of benzothiophene in isooctane by CuY zeolite with different amount of Cu^{2+} loading

The experimental data of the adsorption of BT in isooctane on NiY and CuY zeolites were found to be fitted by Langmuir isotherm. The Langmuir parameters were illustrated in Table 4.4 and Table 4.5 for NiY zeolite and CuY

zeolite, respectively. The NiY zeolite isotherms were not much different when compared with NaY zeolite isotherm. In contrast to the NiY zeolite isotherms, the CuY zeolite isotherms were shifted up when the amount of Cu^{2+} loading on zeolite increased. Although the maximum capacities in adsorbing BT in isooctane of both zeolites were less than the maximum capacities in adsorbing 3-MT in isooctane, k values of the former were higher which contributed to the stronger interaction between BT and both zeolites than 3-MT. It is due to the fact that BT has more electron density of S atoms than 3-MT which cause BT to greatly interact with transition metals (Ni^{2+}, Cu^{2+}) via π-complexation. The k values increased when increasing the amount of Cu^{2+} loading. This indicates that Cu^{2+} can improve the interaction between BT and adsorbents.

Table 4.4 Maximum capacity and adsorption constant of the adsorption of benzothiophene in isooctane by NiY zeolite with different Ni^{2+} loading

Adsorbent	q_{max} (mmol-S/g-orbent)	k (g-fuel/μmol-S)
NiY (2.36%wt Ni)	1.046	1.077
NiY (4.51%wt Ni)	1.143	0.738
NiY (5.38%wt Ni)	1.116	0.930
NaY	0.947	1.515

Table 4.5 Maximum capacity and adsorption constant of the adsorption of benzothiophene in isooctane by CuY zeolite with different Cu^{2+} loading

Adsorbent	q_{max} (mmol-S/g-orbent)	k (g-fuel/μmol-S)
CuY (2.83%wt Cu)	1.013	1.354
CuY (5.18%wt Cu)	0.919	7.583
CuY (6.73%wt Cu)	0.951	11.840
NaY	0.947	1.515

4.2.1.3 Adsorption of dibenzothiophene in decane by NiY and CuY zeolites

In this study, the adsorption isotherm of dibenzothiophene in decane was constructed between the amount of dibenzothiophene adsorbed on zeolite and equilibrium concentration of dibenzothiophene in decane. Fuel:adsorbent ratio

was fixed at 85 and the experiment was carried out at ambient condition. The results are shown in Figure 4.8 and Figure 4.9

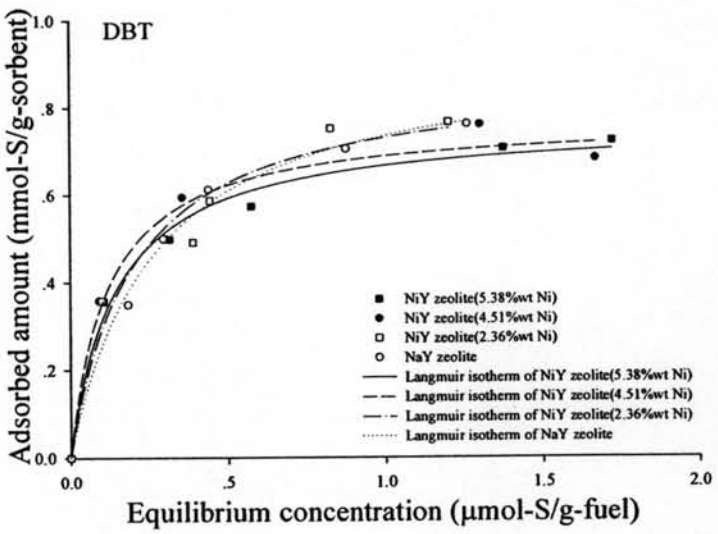

Figure 4.8 Adsorption isotherms of dibenzothiophene in decane by Y zeolite with different amount of Ni^{2+} loading

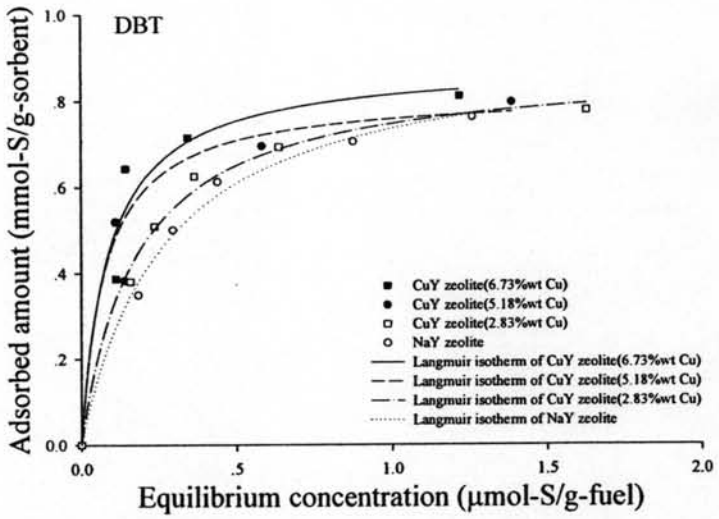

Figure 4.9 Adsorption isotherm of dibenzothiophene in decane in different amount of Cu^{2+} loading on zeolite

From Figures 4.8 and 4.9, the experimental were found to be exhibited the Langmuir isotherm. The Langmuir parameters are shown in Tables 4.6 and 4.7 for NiY and CuY zeolites, respectively. The maximum capacities of NiY zeolite were not significantly different when varying the amount of Ni^{2+} loading which is the same with CuY zeolite. Althouth the k value is higher when increasing the amount of metal loading, they are still lower than CuY zeolite. The maximum capacities in adsorbing DBT in decane were the lowest because of the structural hindrance from the size of molecule which make it is difficult to pass through the pore of zeolites when compared with 3-MT or BT. For adsorption equilibrium constant, k values, in adsorbing DBT is the highest because a high electron density from aromatic rings can strongly interact with transition metals (Ni^{2+}, Cu^{2+}) via π-complexation.

Table 4.6 Maximum capacity and adsorption constant of the adsorption of dibenzothiophene in decane by NiY zeolite with different Ni^{2+} loading

Adsorbent	q_{max} (mmol-S/g-orbent)	k (g-fuel/μmol-S)
NiY (2.36%wt Ni)	0.876	5.046
NiY (4.51%wt Ni)	0.769	8.425
NiY (5.38%wt Ni)	0.762	6.984
NaY	0.928	3.810

Table 4.7 Maximum capacity and adsorption constant of the adsorption of dibenzothiophene in decane by CuY zeolite with different Cu^{2+} loading

Adsorbent	q_{max} (mmol-S/g-orbent)	k (g-fuel/μmol-S)
CuY (2.83%wt Cu)	0.876	5.747
CuY (5.18%wt Cu)	0.815	13.320
CuY (6.73%wt Cu)	0.882	11.720
NaY	0.928	3.810

4.2.2 The Effect of the Types of Sulfur Compounds in Adsorption

To study the effect of the types of sulfur compounds in adsorption of 3-methylthiophene, benzothiophene in isooctane and dibenzothiophene in decane by NiY and CuY, the Lagmuir isotherms of different sulfur compounds were plotted together. The results are demonstrated in Figures 4.10 and 4.11 for NiY zeolite and CuY zeolite, respectively.

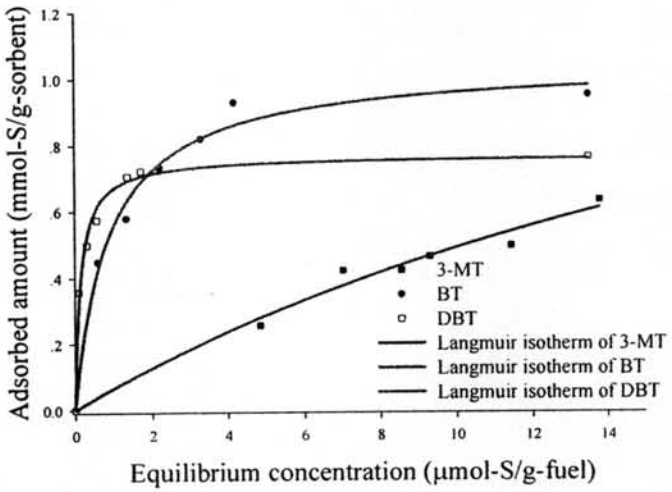

Figure 4.10 The Langmuir isotherms with different sulfur compounds on NiY zeolite

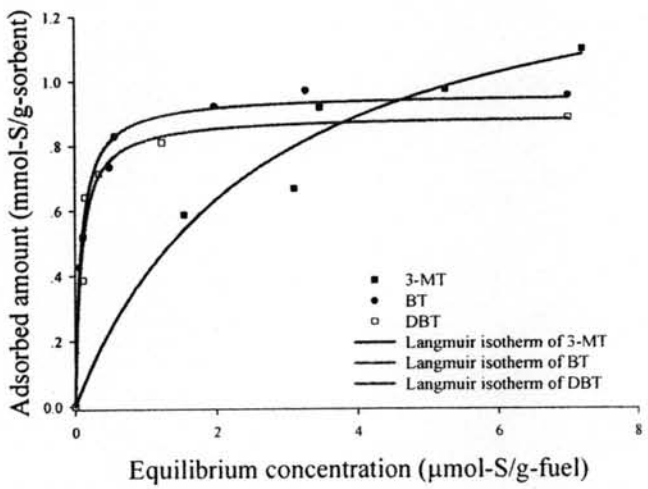

Figure 4.11 The Langmuir isotherms with different sulfur compounds on CuY zeolite

From the isotherms, it can be seen that the slope of DBT and BT isotherms are very steep and much steeper than that of 3-MT isotherms. This is attributed to the benzene ring in the structure of DBT and BT which can form p-bond with the zeolite stronger than 3-MT. In adsorption isotherms of CuY zeolite, DBT show the lowest adsorption capacity which probably due to steric hinderance since DBT has the largest molecular size.

4.3 Adsorption in the Presence of Supercritical Fluids

4.3.1 Mathematical Explanation of Adsorption Equilibria in Supercritical Fluids

The difficulty of experiment of adsorption in the presence of supercritical fluids because it is expensive from the high pressure operation and difficult to handling makes modeling and prediction of the adsorption equilibria in the presence of supercritical fluids become important. It is simplified by translating the parameters in the model in order to fit with the Langmuir isotherm.

The Langmuir isotherm can be described by

$$\frac{q}{q_\infty} = \frac{BC_e}{1+BC_e} \tag{2.3}$$

where $K_i = Bq_\infty$ is the adsorption equilibrium constant of i species in the adsorbed phase. B and q_∞ are the Langmuir constant and saturation capacity, respectively. These constants can be obtained from fitting with experimental data of which may face with the lack in the entire range of concentration. Therefore, the theoretical value of q_∞ was generated by

$$q_\infty = \frac{S_g}{1.09 N_0^{1/3} V^{2/3}} \tag{2.4}$$

where S_g, N_0, and V are the specific surface area of adsorbent, Avogadro's number and molar volume, respectively (Smith, 1981).

For linear chromatography, k_i is defined as (Kelly and Chimowitz, 1990)

$$k_i = \frac{\text{number of moles of solute in the stationary phase}}{\text{number of moles of solute in the mobile phase}}$$

$$= \frac{\rho_B q_i^*}{\varepsilon y_i \rho_m}$$

where $q_i^* / y_i \rho_m$ can be defined as adsorption equilibrium constant (k_i). Thus, this term is expressed by

$$k_i = \frac{K_2 \rho_B}{\varepsilon} \tag{2.5}$$

The derivative fugacity of solute in each phase in equilibrium can be expressed by

$$d \ln f_2^m = d \ln f_2^s$$

where subscript 2 refers to solute and superscript m and s are mobile phase and solid phase, respectively (Kelly and Chimowitz, 1990). By solving the differential equation of the logarithm of the fugacity of the solute in each phase, the temperature dependence at constant pressure and pressure dependence at constant temperature of K_2 can be obtained as expressed in equation (2.6) and (2.7)

$$\left(\frac{\partial \ln K_2}{\partial T}\right)_p = \frac{(h_2^{IG} - \hbar_2^m) + \Delta H_2^{ads}}{RT^2} + \alpha^m \tag{2.6}$$

$$\left(\frac{\partial \ln K_2}{\partial P}\right)_T = \frac{\bar{\upsilon}_2^m}{RT} - \kappa^m \tag{2.7}$$

where heat of adsorption of solute on adsorbents $\Delta H_2^{ads} = \hbar_2^s - h_2^{IG}$ in which $\hbar_2^s$ and $\hbar_2^m$ are partial molar enthalpy at infinite dilution of a solute in the stationary phase and fluid phase, respectively. h_2^{IG} is the enthalpy of solute in the ideal gas state. υ_2^m represents partial molar volume at infinite dilution of a solute in the mobile phase as well as α^m and κ^m are volume expansivity and the isothermal compressibility of the fluid phase. The heat of adsorption is independent of the chemical structure of the solute due to the interaction between the solute molecules and the adsorbent are weak van der Waals forces.

The residual infinite-dilution partial molar enthalpy $(h_2^{IG} - \hbar_2^m)$, $\bar{\upsilon}_2^m$, α^m, κ^m can be calculated by using Peng-Robinson equation of state with van der Waals mixing rules which can be expressed by (Jha and Madras, 2004)

$$\alpha^m = \frac{1}{V}\left(\frac{\partial V}{\partial T}\right)_{p,y} = \frac{\dfrac{\partial a/\partial T}{V\left(V^2+2Vb-b^2\right)} - \dfrac{R}{\left(V\left(V-b\right)\right)}}{\dfrac{2a\left(V+b\right)}{\left(V^2+2Vb-b^2\right)^2} - \dfrac{RT}{\left(V-b\right)^2}} \tag{2.8}$$

$$\kappa^m = -\frac{1}{V}\left(\frac{\partial V}{\partial p}\right)_{T,y} = \frac{1}{\left(-2a\left(V+b\right)V/\left(V^2+2Vb-b^2\right)^2\right)+RTV/\left(V-b\right)^2} \tag{2.9}$$

$$\bar{\upsilon}_i^m = \kappa^m V\left[\frac{V-b+B}{\left(V-b\right)^2} - \frac{\left(V^2+2Vb-b^2\right)A-2a\left(V-b\right)B}{\left(V^2+2Vb-b^2\right)^2}\right] \tag{2.10}$$

$$\begin{aligned}\hbar_i^m - h_i^{IG} = {} & p\bar{\upsilon}_i^m - RT + \frac{\left(T\left(\partial a/\partial T\right)-a\right)\left(VB-b\bar{\upsilon}_i^m\right)}{b\left(V^2+2Vb-b^2\right)} \\ & + \frac{1}{2\sqrt{2}b}\ln\left(\frac{V+\left(1-\sqrt{2}\right)b}{V+\left(1+\sqrt{2}\right)b}\right)\left[\frac{T}{n}\left(\frac{\partial^2 n^2 a}{\partial T\partial n_i}\right) - A - \frac{1}{b}\left(T\frac{\partial a}{\partial T}-a\right)B\right]\end{aligned} \tag{2.11}$$

where

$$A = \frac{1}{n}\frac{\partial n^2 a}{\partial n_i},\quad B = \frac{\partial nb}{\partial n_i}$$

n and n_i represent total number of moles and number of moles of i*th* species.

The Peng-Robinson equation of state (Peng and Robinson, 1976) is

$$p = \frac{RT}{V-b} - \frac{a}{V^2+2Vb-b^2} \tag{2.12}$$

where a and b are the parameters in the equation of state which can be estimated from

$$a = \frac{0.457235R^2T_c^2\gamma}{p_c} \tag{2.13}$$

$$\gamma = \left(1+\left(0.37464+1.54226\omega-0.26992\omega^2\right)\left(1-\sqrt{T/T_c}\right)\right) \tag{2.14}$$

$$b = \frac{0.07779RT_c}{p_c} \tag{2.15}$$

for pure components and for binary components, classical van der Waals mixing rules were applied

$$a = \sum_i^n \sum_j^n x_i x_j a_{ij} \quad \text{and} \quad b = \sum_i^n \sum_j^n x_i x_j b_{ij} \tag{2.16}$$

with combining rules of Kwak and Mansoori (1986)

$$a_{ij} = (1 - k_{ij})\sqrt{a_{ii} a_{jj}} \tag{2.17}$$

$$b_{ij} = (1 - l_{ij})\frac{\left(b_{ii}^{1/3} + b_{jj}^{1/3}\right)^3}{8} \tag{2.18}$$

a_{ii}, a_{jj}, b_{ii} and b_{jj} are the paramerters of equation of state of pure components i and j. k_{ij} and l_{ij} are binary interaction parameters determined by regressing experimental data of P-x isotherm with Peng-Robinson equation of state as described by Byun and Lee (2006), Kwon *et al.* (2005), and Kwon *et al.* (2007). The objective function (OBJ) and the root-mean-squared relative deviation (RMSD) of this calculation can be defined as follow:

$$OBJ = \sum_i^N \left(\frac{p_{\exp} - p_{cal}}{p_{\exp}} \right)^2 \tag{2.19}$$

$$RMSD = \sqrt{\frac{OBF}{ND}} \times 100 \tag{2.20}$$

The subscript *exp* and *cal* are experimental results and calculated results, respectively. ND means the number of data points.

4.3.2 Prediction of Interaction Parameters in Kwak and Mansoori Mixing Rule

The difficulty of experiment of adsorption in the presence of supercritical fluids because it is expensive from the high pressure operation and difficult to handling makes modeling and prediction of the adsorption equilibria in the presence of supercritical fluids become important. The Peng-Robinson model was usually used in adsorption equilibria. One thing that can make a precision of Peng-Robinson model is the determination of interaction parameters in combining rule when mixing rule was applied for binary components. The experiment selected

to verify the model written by FORTRAN program is CO_2 + 2,2,2-Trifluoroethyl Methacrylate System (Kwon *et al.*, 2007). The binary interaction parameters were determined by regression the experimental data by Peng-Robinson equation by minimizing the objective function ($\sum_{i}^{N}\left(\frac{p_{exp}-p_{cal}}{p_{exp}}\right)^2$). From their experiment, the interaction parameters k_{ij} and l_{ij} were -0.0258 and -0.0234, respectively. In simulation written by FORTRAN, the interaction parameters k_{ij} and l_{ij} were -0.0235 (8.91% deviation) and -0.0244 (4.27% deviation), respectively. The values from FORTRAN have relatively low deviation. Thus, this program can be used in other systems.